Materials Physics and Mechanics. 2022;50(2): 342-354
Research article
http://dx.doi.org/10.18149/MPM.5022022_13

Submitted: July 7, 2022
Approved: August 23, 2022
Accepted: August 29, 2022

Principal stress-strain states of thin-walled complexly bent pipelines

O.P. Tkachenko✉

Computing Center of the Far Eastern Branch of the Russian Academy of Sciences, Kim Yu Chen Str., 65, Khabarovsk, 680000, Russia

✉olegt1964@gmail.com

Abstract. Mathematical model of the pipeline is formulated within the framework of the elastic shell theory, and the basic parameters of this model are determined. For moment and semi-momentless shells, equations of the first approximation with respect to the small curvature parameter are given. The model for calculation by the finite element method in CAE Abaqus is constructed and numerical experiments are performed. Numerical solution to the model problem is found, and stresses and bending moments are calculated on its basis. Stresses and bending moments are compared with their exact values. Numerical analysis is carried out by comparing pipe models within the framework of the shell theory and the rod theory. It is established that the proposed mathematical model makes it possible to find stresses in pipes with high accuracy.

Keywords: numerical experiment, thin-walled shells, mathematical model, adequacy estimates

Acknowledgements*. The work has been supported by the Russian Science Foundation grant № 21-11-00039, https://rscf.ru/en/project/21-11-00039/*

Citation: Tkachenko OP. Principal stress-strain states of thin-walled complexly bent pipelines. *Materials Physics and Mechanics*. 2022;50(2): 342-354. DOI: 10.18149/MPM.5022022_13.

1. Introduction

With the development of oil and gas fields on the sea shelf, engineers around the world are faced with a problem: pipelines are displaced from their design position [1]. Engineers and scientists are actively developing methods to prevent lateral and vertical displacement of subsea pipelines [2]. Various reasons for such a displacement are studied in [3,4]. Engineering methods for designing underwater pipelines, taking into account their instability, have been included in textbooks (see, for example, [5]), but this fact does not remove the problem of the unexplored phenomena.

In this regard, the question arises of choosing a mathematical model of the pipeline for further analysis of its behavior under various external loads. Rod models are applied for very long pipes [6]. For pipes of medium length, the shell model is adequate (see [7]). The applicability areas of the rod and the shell models are compared in [8]. This is done on the example of the pipeline tunneling problem. It turns out that for underground pipelines there are conditions in which the rod theory approximation is inapplicable due to the fact that the problem is fundamentally three-dimensional [9].

Previously, we have developed mathematical models both in the framework of the shell theory [10] and the rod theory [11]. An asymptotic analysis of the shell dynamics equations is performed, and an algorithm for reducing the initial-boundary value problem to a one-dimensional formulation is developed on the basis of this analysis [12]. The model of a semi-momentless shell is generalized to moment shells of medium thickness in [13]. In the articles [12,13], a numerical method for solving the resulting systems of equations is proposed and its verification is performed.

The purpose of this research is a comparative analysis of mathematical models of the pipeline, finding areas of their application, and verification of the moment shell model by stresses.

The formulation of the general mathematical model for the pipeline is given and the basic parameters of this model are determined. For moment and semi-momentless shells, equations of the first approximation with respect to the small curvature parameter are given. For the model problem of bending a pipeline segment, the acting forces and stresses are calculated. Numerical solution of the model problem is found, stresses and bending moments are calculated on its basis. Model is constructed for finite element method analysis in CAE Abaqus. Stresses and bending moments are compared with their exact values. It is established that the proposed mathematical model makes it possible to find stresses in pipes with high accuracy. Numerical analysis is performed to compare the application areas of the pipe models as the shell and the rod.

2. Formulation of the pipeline mathematical model

A bent segment of the pipeline is considered, which is under the action of fluid pressure and the centrifugal force of the flow inertia. Within the framework of this work, the stress-strain state of the pipe wall is described by the equations of an elastic shell. The curvilinear coordinate system s, θ, and R is described in [12]. It is assumed that the center line Γ is a flat curve of length L. A natural arc of length s is plotted along the axial line, and a polar coordinate system (θ, R) is constructed at each point of the arc.

The model is based on the equations of V.Z. Vlasov [14]:

$$\frac{1}{A}\left(\frac{\partial I_0}{\partial s}+\frac{h^2}{6}H\frac{\partial I_1}{\partial s}+\frac{h^2}{12}\frac{\partial I_2}{\partial s}\right)-(1-\nu)\frac{1}{B}\left(\frac{\partial X_0}{\partial \theta}+\frac{h^2}{6}k_1\frac{\partial X_1}{\partial \theta}+\frac{h^2}{12}\frac{\partial X_2}{\partial \theta}\right)+$$

$$+(1-\nu)\left(Ku-\frac{k_2}{A}\frac{\partial w}{\partial s}\right)=-\frac{1-\nu^2}{Eh}X,$$

$$\frac{1}{B}\left(\frac{\partial I_0}{\partial \theta}+\frac{h^2}{6}H\frac{\partial I_1}{\partial \theta}+\frac{h^2}{12}\frac{\partial I_2}{\partial \theta}\right)+(1-\nu)\frac{1}{A}\left(\frac{\partial X_0}{\partial s}+\frac{h^2}{6}k_2\frac{\partial X_1}{\partial s}+\frac{h^2}{12}\frac{\partial X_2}{\partial s}\right)+$$

$$+(1-\nu)\left(K\nu-\frac{k_1}{B}\frac{\partial w}{\partial \theta}\right)=-\frac{1-\nu^2}{Eh}Y, \qquad (1)$$

$$-2H\cdot I_0-\frac{h^2}{6}\left(HI_2+KI_1\right)+\frac{h^2}{12}\frac{1}{AB}\left\{\frac{\partial}{\partial s}\left[\frac{B}{A}\left(k_2\frac{\partial I_0}{\partial s}+\frac{\partial I_1}{\partial s}-(1-\nu)K\frac{\partial w}{\partial s}\right)-(1-\nu)k_1\frac{\partial X_0}{\partial \theta}\right]+\right.$$

$$\left.+\frac{\partial}{\partial \theta}\left[\frac{A}{B}\left(k_1\frac{\partial I_0}{\partial \theta}+\frac{\partial I_1}{\partial \theta}-(1-\nu)K\frac{\partial w}{\partial \theta}\right)+(1-\nu)k_2\frac{\partial X_0}{\partial s}\right]\right\}+$$

$$+\frac{h^2}{12}\frac{(1-\nu)}{AB}\left[\frac{\partial}{\partial s}(BKk_1u)+\frac{\partial}{\partial \theta}(AKk_2\nu)\right]+\frac{1-\nu}{AB}\left[2ABKw+\frac{\partial}{\partial s}(Bk_2u)+\frac{\partial}{\partial \theta}(Ak_1\nu)\right]=-\frac{1-\nu^2}{Eh}Z.$$

In system (1) it is denoted:

$K = k_1 k_2$, $\mathrm{H} = \frac{1}{2}(k_1 + k_2)$, $L = \frac{1}{2}(k_1 - k_2)$;

X, Y, and Z are loads acting on the pipe along the coordinates s, θ, and R, respectively; v is Poisson's ratio, E is Young's modulus, h, R_0 are wall thickness and radius of the middle surface of the pipe, respectively, u, v, w are displacements of the middle surface along the coordinate axes, k_1, k_2 – principal curvatures of the middle surface. Generalized expressions for functions I_i, X_i in terms of displacements, where $i = 0,1,2$, are given in [14].

Denote by $\kappa(s)$ the curvature of the pipe axial line; in the position before deformation, it is equal to $\kappa_0(s)$. Conditions for applicability of the shell theory are:

$$h^* = \frac{h}{R_0} \le 1/20, \quad \frac{\min\left(L,\ 1/\kappa_0\right)}{R_0} \ge 4, \tag{2}$$

The geometric parameters of equations (1) are expressed by formulas:

$A = 1 + R_0 \kappa(s) \sin\theta$, $B = R_0$,

$k_1 = \kappa(s) \sin\theta \,/\left(1 + \kappa(s) R_0 \sin\theta\right)$, $k_2 = 1/R_0$.

Substituting these expressions into (1), and expressing all the terms in terms of wall displacements, we obtain three equations for three unknown displacements. Introducing dimensionless coordinates and functions:

$\zeta = s/\ell$; $\quad r = R/R_0$; $\quad \theta = \theta$;

$u' = u/R_0$; $\quad v' = v/R_0$; $\quad w' = w/R_0$;

we bring the resulting system of resolving equations to a dimensionless form. Here ℓ is the characteristic scale. The resulting equations are published in [13]; they are not presented here due to their cumbersomeness.

The pipeline geometry is determined by the curvature parameter:

$\lambda = R_0 \max|\kappa_0|$.

This parameter characterizes the degree of pipe bending. The boundary value problem for a pipe with a kink, when $\lambda \to \infty$, is considered in [15]. For the numerical solution of this problem, which contains a singularity in its coefficients, new methods are being developed in [16-18]. A review of dynamic problems of crack propagation in pipeline walls, which also contain a singularity, is presented in [19].

It is assumed that the inequality performed

$$\lambda \le 1/20, \tag{3}$$

which is related to inequalities (2). Inequality (3) allows us to use the smallness of the parameter λ.

3. First approximation equations

The system of equations (1) admits various degrees of approximation. In [12,13], two mathematical models are proposed: one based on the semi-momentum theory of shells in [12] and one based on the moment theory of shells in [13]. It is proved in [13] that there are such conditions for applying the load on the pipe that in both cases the same expansion in powers of a small parameter is applicable:

$$\begin{aligned} u'(\zeta,\theta) &= u_0(\zeta) + \lambda u_1(\zeta)\sin\theta + O\left(\lambda^2\right); \\ v'(\zeta,\theta) &= \lambda v_2(\zeta)\cos\theta + O\left(\lambda^2\right); \\ w'(\zeta,\theta) &= w_0(\zeta) + \lambda w_1(\zeta)\sin\theta + O\left(\lambda^2\right). \end{aligned} \tag{4}$$

Here the dimensionless variables are introduced, which are defined above. The result of substituting (4) into different models from [12] and [13] differs in the first approximation.

First order resolving equations for a bent shell of medium thickness have the following form:

$$\alpha^2 u_{1\zeta\zeta} + \alpha\nu w_{1\zeta} - \varepsilon^2\alpha^3 w_{1\zeta\zeta\zeta} - \frac{1+\nu}{2}\alpha v_{2\zeta} - \frac{1-\nu}{2}u_1 = f_1;$$

$$-w_1 + v_2 - \nu\alpha u_{1\zeta} + \varepsilon^2\left[-\alpha^4 w_{1\zeta\zeta\zeta\zeta} + 2\alpha^2 w_{1\zeta\zeta} + \frac{\nu-3}{2}\alpha^2 v_{2\zeta\zeta} + \alpha^3 u_{1\zeta\zeta\zeta}\right] = f_2;$$

$$\frac{1-\nu}{2}\alpha^2 v_{2\zeta\zeta} - v_2 + \frac{1+\nu}{2}\alpha u_{1\zeta} + w_1 - \varepsilon^2\alpha^2\frac{3-\nu}{2}w_{1\zeta\zeta} = f_3; \qquad (5)$$

$$f_1 = 2\alpha^2 f u_{0\zeta\zeta} + \alpha^2 f_\zeta u_{0\zeta} - \alpha f_\zeta w_0 - \alpha\left[(1-\nu) f + \varepsilon^2\alpha^2 f_{\zeta\zeta}\right]w_{0\zeta} -$$

$$-\left(\frac{1-\nu}{2} f + \varepsilon^2\alpha^2 f_{\zeta\zeta}\right)u_0 - \varepsilon^2\alpha^3\left(4 f_\zeta w_{0\zeta\zeta} + 3 f w_{0\zeta\zeta\zeta}\right) - X_1 \,/\, E^* h^*;$$

$$f_2 = \left(2\nu f - \varepsilon^2\alpha^2 f_{\zeta\zeta}\right)w_0 + \left[(1-\nu) f - \varepsilon^2\alpha^2 f_{\zeta\zeta}\right]\alpha u_{0\zeta} - \varepsilon^2\left[4\alpha^4 f w_{0\zeta\zeta\zeta\zeta} +\right.$$

$$+6\alpha^4 f_\zeta w_{0\zeta\zeta\zeta} - \left[(1-\nu) f - 4\alpha^2 f_{\zeta\zeta}\right]\alpha^2 w_{0\zeta\zeta} + \left(\nu f_\zeta + \alpha^2 f_{\zeta\zeta\zeta}\right)\alpha^2 w_{0\zeta} -$$

$$\left.-3\alpha^3 f u_{0\zeta\zeta\zeta} - 2\alpha^3 f_\zeta u_{0\zeta\zeta} - \frac{\alpha}{2}\left[(1+\nu) f_\zeta - 2\alpha^2 f_{\zeta\zeta\zeta}\right]u_0\right] - Z_1^1 \,/\, E^* h^*;$$

$$f_3 = -\frac{\nu-3}{2}\alpha f u_{0\zeta} - \frac{\nu-1}{2}\alpha f_\zeta u_0 - f w_0 -$$

$$-\varepsilon^2\frac{\alpha^2}{2}\left[(3-\nu) f_\zeta w_{0\zeta} + (7-\nu) f w_{0\zeta\zeta}\right] - Y_2^1 \,/\, E^* h^*.$$

First-order resolving equations for a thin-walled semi-momentless shell have the following form:

$$\alpha^2 u_{1\zeta\zeta} - \frac{1-\nu}{2}u_1 - \frac{1+\nu}{2}\alpha v_{2\zeta} + \nu\alpha w_{1\zeta} + f\left[\frac{1-\nu}{2}u_0 - 2\alpha^2 u_{0\zeta\zeta} + \alpha(1-\nu)w_{0\zeta}\right] -$$

$$-\alpha^3\left(w_{1\zeta}w_{0\zeta\zeta} + w_{0\zeta}w_{1\zeta\zeta}\right) + 3\alpha^3 f\cdot w_{0\zeta}w_{0\zeta\zeta} = \frac{\rho_t R_0^2\omega^2}{E^*}u_{1\tau\tau}; \qquad (6)$$

$$\frac{1-\nu}{2}\alpha^2 v_{2\zeta\zeta} - v_2 - \frac{1}{E^* h^*}\frac{2u_1^*\mu}{R_0\left(0.5 - \ln\left|\frac{\gamma\rho_e\lambda u_1^*}{4\mu}R_0\right|\right)} + \frac{1+\nu}{2}\alpha u_{1\zeta} +$$

$$+w_1 + f\left(w_0 - \frac{3-\nu}{2}\alpha u_{0\zeta}\right) - \alpha^2 w_{0\zeta}w_{1\zeta} = \frac{\rho_t R_0^2\omega^2}{E^*}v_{2\tau\tau};$$

$$w_1 + \frac{h^{*2}}{12}\left(\alpha^4 w_{1\zeta\zeta\zeta\zeta} - \alpha^2 w_{1\zeta\zeta}\right) + \nu\alpha u_{1\zeta} - v_2 +$$

$$+f\left[2\nu w_0 + (1-\nu)\alpha u_{0\zeta}\right] - \alpha^2 w_{0\zeta}w_{1\zeta} +$$

$$+\frac{\alpha^2}{2} f\left(w_{0\zeta}\right)^2 = \frac{1}{E^* h^*}\left[\rho_f\vartheta_{s0}^2 f - \frac{2u_1^*\mu}{R_0\left(0.5 - \ln\left|\frac{\gamma\rho_e\lambda u_1^*}{4\mu}R_0\right|\right)}\right] - \frac{\rho_t R_0^2\omega^2}{E^*}w_{1\tau\tau}.$$

Here denoted:

$E^* = E/\left(1-\nu^2\right)$, $\varepsilon^2 = h^{*2}/12$, $\alpha = R_0/\ell$, $f = \kappa/\max|\kappa|$.

By subscripts ζ, τ denote differentiation with respect to the corresponding variable.

The boundary conditions for the systems of equations are identical and imply hinged pipe edges:

$$u_1 = v_2 = w_1 = 0;\ \frac{\partial^2 w_1}{\partial \zeta^2} = 0, \text{ for } \zeta = 0;$$
$$u_1 = v_2 = w_1 = 0;\ \frac{\partial^2 w_1}{\partial \zeta^2} = 0, \text{ for } \zeta = L'. \tag{7}$$

Comparing equations (5) and (6), one can find that the left-hand sides of equations (5) contain additional terms with third-order derivatives. This makes the order of the equations system (5) higher than the order of system (6).

4. Methods and algorithms for the numerical solution of problems

Parameters λ, h^*, E_{irv} are taken as the defining parameters of mathematical models. An analogue of the Irwin parameter [20] is defined in [21]:

$$E_{irv} = \sqrt{\frac{2hE}{\beta\left(R_0 - h/2\right)Lv_{s0}^2}}, \tag{8}$$

where β is the friction coefficient of the flow in the pipe [22].

The constraint on the parameter h^* is established by relations (2). Based on the data of [14], it can be argued that for the applicability of the mathematical model of a semi-momentless shell, a stronger constraint must be satisfied:

$$h^* \le 1/30.$$

If restrictions (2) and restrictions on the parameter E_{irv} are not met, then it is necessary to use the rod model of the pipe, for example, described in [11], or use the medium-thickness shell model described in [14].

For the numerical analysis of problems (6) and (7), a computer program is created in the FORTRAN language, the operation algorithm and the numerical method of which are described in [12]. The numerical solution to problems (5) and (7) can be found using the algorithm described in [13].

Here we will verify and refine the scope of models [12,13] based on their numerical analysis by the finite element method in CAE Abacus [23]. We also use the MATLAB application package to analyze the errors that are introduced in the numerical analysis of the created models in the calculation of bending moments and stresses in the pipe wall. We will also perform numerical experiments to clarify the areas of applicability of mathematical models of the pipeline as the rod and as the shell.

5. Tasks for verifying mathematical model

Task 1. The classic problem of S.P. Timoshenko about a bent pipe under a distributed load [24] is chosen as a test one. A slightly curved beam under a distributed load q_n is considered. Let us define the initial undeformed line of the beam by the function

$$y_0 = b_1 \sin\frac{\pi z}{L}. \tag{9}$$

Let the deflection be described by the function

$$y - y_0 = a_1 \sin\frac{\pi z}{L}.$$

This formula corresponds to the first term of the expansion of the solution in a Fourier series on the interval $[0, L]$, and accurately describes the beam deflection, according to [24]. It is easy to find that for a given geometry:

$$\lambda = \pi^2 \frac{R_0 b_1}{L^2}.$$

Establishing a correspondence between the bending line of the beam and the displacement of the pipe centerline as a shell, we find that for the model problem the exact solution of equations (1) has the form:

$$u' = \lambda \frac{a_1 L}{\pi R_0 b_1} \cos\left(\frac{\pi\zeta}{L'}\right) \sin\theta,$$

$$v' = -\lambda \frac{a_1 L^2}{\pi^2 R_0^2 b_1} \sin\left(\frac{\pi\zeta}{L'}\right) \cos\theta,$$

$$w' = -\lambda \frac{a_1 L^2}{\pi^2 R_0^2 b_1} \sin\left(\frac{\pi\zeta}{L'}\right) \sin\theta.$$

The boundary conditions for this solution should have the form:

$$\begin{aligned} &u' = \lambda \frac{a_1 L}{\pi R_0 b_1} \sin\theta,\ v' = 0,\ w' = 0, \quad \frac{\partial^2 w'}{\partial \zeta^2} = 0 \quad \text{for} \quad \zeta = 0; \\ &u' = -\lambda \frac{a_1 L}{\pi R_0 b_1} \sin\theta,\ v' = 0,\ w' = 0, \quad \frac{\partial^2 w'}{\partial \zeta^2} = 0 \quad \text{for} \quad \zeta = L'. \end{aligned} \tag{10}$$

The zero approximation functions for both models (5) and (6) vanish. The exact first-order solutions for these models coincide and have the form:

$$u_1(\zeta) = \frac{a_1 L}{\pi R_0 b_1} \cos\left(\frac{\pi\zeta}{L'}\right);$$

$$v_2(\zeta) = -\frac{a_1 L^2}{\pi^2 R_0^2 b_1} \sin\left(\frac{\pi\zeta}{L'}\right);$$

$$w_1(\zeta) = -\frac{a_1 L^2}{\pi^2 R_0^2 b_1} \sin\left(\frac{\pi\zeta}{L'}\right).$$

The right parts for the semi-momentless shell (6) have the form:

$$f_1 = -\frac{a_1}{b_1} \frac{\pi R_0}{L} \cos\frac{\pi\zeta}{L'}; \quad f_2 = -\nu \frac{a_1}{b_1} \sin\frac{\pi\zeta}{L'};$$

$$f_3 = -\nu \frac{a_1}{b_1} \sin\frac{\pi\zeta}{L'} + \varepsilon^2 \left(\frac{\pi^2 R_0^2}{L^2} + 1\right) \frac{a_1}{b_1} \sin\frac{\pi\zeta}{L'}.$$

Right-hand sides for the moment shell (5) have the form:

$$f_1 = -\frac{a_1}{b_1} \frac{\pi R_0}{L} \cos\frac{\pi\zeta}{L'} - \varepsilon^2 \frac{a_1}{b_1} \frac{\pi R_0}{L} \cos\frac{\pi\zeta}{L'};$$

$$f_2 = \nu \frac{a_1}{b_1} \sin\frac{\pi\zeta}{L'} + \varepsilon^2 \left(\frac{2\pi^2 R_0^2}{L^2} + \frac{1+\nu}{2}\right) \frac{a_1}{b_1} \sin\frac{\pi\zeta}{L'};$$

$$f_3 = -\nu \frac{a_1}{b_1} \sin\frac{\pi\zeta}{L'} - \varepsilon^2 \frac{3-\nu}{2} \frac{a_1}{b_1} \sin\frac{\pi\zeta}{L'}.$$

The accuracy of the mathematical model (6) is estimated in [12]. We present here the results of numerical experiments to assess the accuracy of finding the bending moments and stresses using the mathematical model (5) with boundary conditions (10).

Numerical data of the model task are: $b_1 = 5.0$ m, $h = 0.01$ m, $L = 120$ m, $R_0 = 0.2$ m, $E = 2.07 \cdot 10^5$ MPa, $\nu = 0.24$, $V_{s0} = 1$ m/s, $\rho_f = 998$ kg/m^3, $\rho_t = 7200$ kg/m^3, $\ell = 1$ m, $S_f = 0.1195$ m^2.

Here denoted: V_{s0} is fluid flow velocity, ρ_f is fluid density, ρ_t is pipe material density, S_f ispipe lumen area.

Task 2. To separate the areas of applicability of the rod model [11] and the thin-walled shell model [12], we choose the dynamic problem of bending an extended pipeline with a profile in the form of a chain. Model parameters are: fluid flow velocity $V_{s0} = 1.5$ m/s, viscosity of the external media $\mu_e = 5000$ Pa·s, fluid viscosity $\mu = 0.1$ Pa·s, wall thickness $h = 0.005$ m, pipe radius $R_0 = 0.23$ m, pipe length $L = 3009$ m. A time interval of 48 hours was calculated.

The chain is a curvewhere the coordinates of the points follow the relation [25]:

$$y = A + B \cdot \cosh\left(\frac{x - x_0}{B} - 1\right).$$

The solution to the problem of finding chain line parameters is known and presented in [25]. In *task 2,* the chain line parameters are as follows: $x_1 = 0$, $y_1 = 0$, $x_2 = 3000$ m, $y_2 = 200$ m, $A = -21901.4$ m, $B = 21901.4$ m, $x_0 = -21859.2$ m. With these parameters, the minimum radius of curvature of the axis is found: $\min |\rho_0| \approx 17092.4$ m.

Methods for the numerical analysis of *task 2* are described in [11,12].

6. Numerical results and discussion

Task 1. As proved in [24], the solution of the stress problem in a slightly bent rod under a distributed load can be well approximated by the solution of the stress problem in a straight beam with the same cross-section. To obtain numerical estimates of bending moments and stresses, we approximately replace the beam of shape (9) with a circle segment with a chord of 120 m and a 5 m lifting boom, in accordance with the numbers given above. The circle radius is found taking into account the concept of the degree of a point *p* for the midpoint of the segment *[0, L]* using the Huygens formula (see [25]). We get radius ρ_0=360 m. Calculating the distributed transverse load on the pipe according to the formula (see [11]):

$$q_n = \frac{\rho_f}{\rho_0} S_f V_{s0}^2,$$

we get $q_n \approx 0.3312$ N/m. This load corresponds to the force P=39.74 N, distributed along the entire length of the beam.

Solving the problem by the strength of materials methods [26], we find the maximum bending moment in absolute value and the corresponding stress:

$$\max |M_x| \approx 596.1 \text{ Nm}, \ \max |\sigma_z| \approx 486 \text{ kPa}.$$

These values of quantities can be guided by the analysis of the numerical experiment results.

This calculation was verified by the finite element method in the APM WIN Machine software package [27]. Tables 1 and 2 contain excerpts from the tables for calculating bending moments and equivalent stresses, containing the maximum modulo values of these quantities.

Thus, in APM WIN Machine it was found that the maximum bending moment modulo is 596.1 Nm. This value coincided with the value obtained by the methods of strength of materials. The maximum value of the equivalent stress is 0.48461 MPa. The relative deviation from the value obtained by the methods of strength of materials is:

$$\max \varepsilon_z = \frac{\max \left| \sigma_z - \sigma_{eq} \right|}{\max \sigma_{eq}} 100\% = 4.1\%.$$

Table 1. Bending moments

Distance (mm)	Bending moment (Nm)
57600.0	-595.14684
58800.0	-595.86216
60000.0	-596.10060
61200.0	-595.86216
62400.0	-595.14684

Table 2. Equivalent stresses

Distance (mm)	Equivalent stress σ_{eq} (MPa)
57600.0	0.48384
58800.0	0.48442
60000.0	0.48461
61200.0	0.48442
62400.0	0.48384

So, the approximate values of bending moments and equivalent stresses are obtained in two different ways. In this case, the stress values differ from each other within the accuracy of the rod theory (see [26]).

Let us denote J_x as the moment of inertia of the pipe cross-section, W_x as the moment of its section resistance relative to the axis Ox. With the above numerical parameters of the model, J_x=0.0002515 m^4, W_x=0.001223 m^3. The bending moment is related to the beam deflection v_n by the formula (see [26]):

$$M_x = EJ_x \frac{d^2 v_n}{dz^2},\ v_n = y - y_0. \tag{11}$$

The stress is related to the bending moment by the relation (see ibid.):

$$\sigma_z = M_x \Big/ W_x. \tag{12}$$

Formulas (11) and (12) are applicable when condition (3) is satisfied. Taking into account the smallness of the curvature κ=1/360 m^{-1} and the equality ℓ=1 m, formula (11) does not change when z is replaced by ζ.

The method for finding a numerical solution to the boundary value problem (5), (7) is described in [13] and implemented in the MATLAB software package. It is also established there that the displacement of the axial line of the pipe is associated with unknown functions by the formula:

$$v_{nh} = -\frac{\lambda R_0}{2}\left(v_{2h} + w_{1h}\right). \tag{13}$$

All changes of variables are already taken into account in (13), and the deflection v_{nh} is expressed in meters.

To find a numerical solution, a grid of equally spaced points ζ_I is constructed, and the index i varies from 1 to 4000. The grid step is h=0.03 m. These parameters are chosen to find the best approximation of the exact solution. Problem (5), (10) with the selected data is a rigid boundary value problem; the bvp5c method of the MATLAB package is used to solve it.

Let us determine the errors in finding the bending moments and stresses by the formulas:

$$\varepsilon_M = \frac{|M_x - M_{xh}|}{\max|M_x|},\ \varepsilon_\sigma = \frac{|\sigma_z - \sigma_{zh}|}{\max|\sigma_z|}.$$

The numerical values of bending moments M_x and normal stresses σ_{zh} on the grid $\{\zeta_i\}$ are found using formulas (11)–(13).

Since the stress σ_z is the main one for a given type of load on the beam (see [26]), the equality $\sigma_{eq} \approx |\sigma_z|$ is actually fulfilled, where σ_{eq} is the von Mises equivalent stress. The absolute values of stresses for exact and numerical solutions are shown in Fig. 1. The figure shows that the exact and approximate stress values are in good agreement.

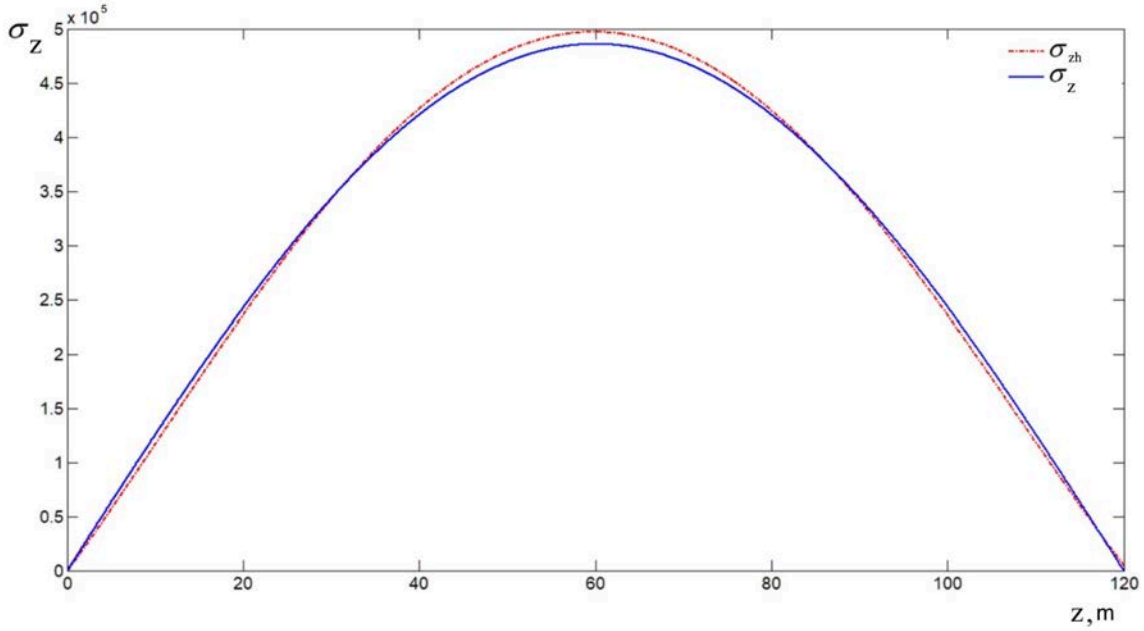

Fig. 1. Modules of maximum stresses in the pipe section, Pa

The quantitative value of the error in the calculation of stresses and moments is given by the analysis of the above-defined values ε_M, ε_σ. These values are shown in Fig. 2.

Maximum error values are: $\max \varepsilon_M = 0.023$, $\max \varepsilon_\sigma = 0.023$.

These results are obtained by approximating the numerical solution v_{2h}, w_{1h} by sixth-order polynomials and using standard MATLAB functions to find derivatives of polynomials.

Let us present the results of the calculation of the same mechanical system by the finite element method in CAE Abaqus. A curved two-bearing beam is built with the geometric parameters of the model problem, loaded with the distributed load q_n=0.3312 N/m calculated above. The construction technique is described in [23].The constructed geometric model contained a one-dimensional FEM grid of 100 elements with a grid step h=1.2 m. The von Mises stresses obtained after the calculations are shown in Fig. 3. It is known [26] that in direct bending of the beam, the equivalent von Mises stress coincides with $|\sigma_z|$, as we obtained in the Abaqus report file.

The maximum value of the stress modulus in the numerical solution in Fig. 1 is $\max|\sigma_z| = 0.49707$ MPa, and the maximum stress in Fig. 3 is $\max\sigma_{eq}$=0.4743 MPa. This numerical value is obtained from the Abaqus report file generated at the end of the calculation.

The graph of the exact solution for stresses as a function of the longitudinal coordinate is shown in Fig. 1. The exact stress values and their numerical approximations in Abaqus are shown in Fig. 4.

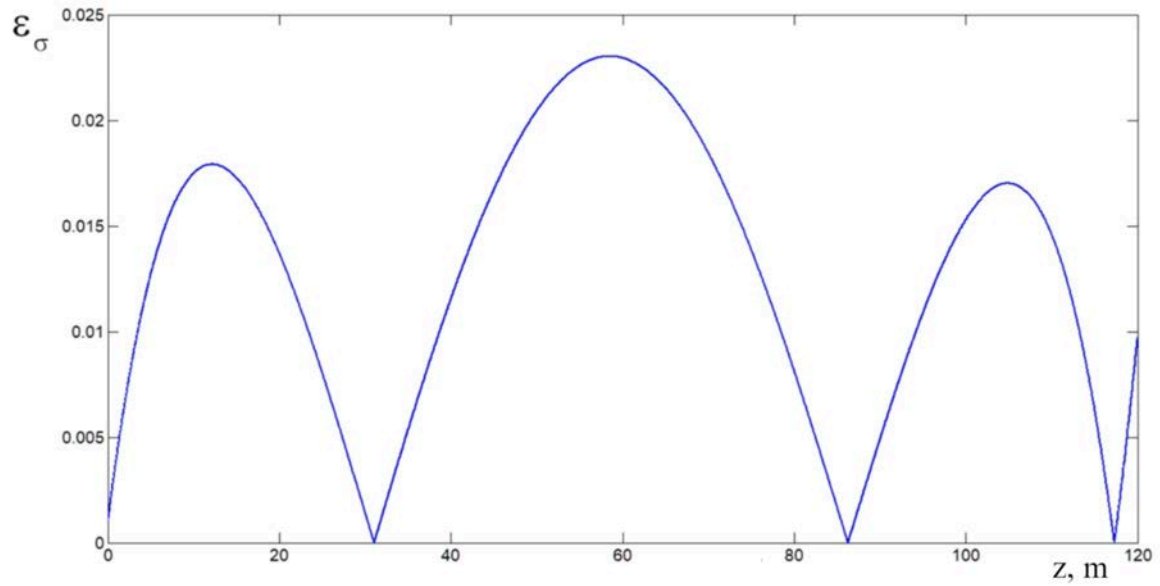

Fig. 2. Error module for calculating stresses in a pipe

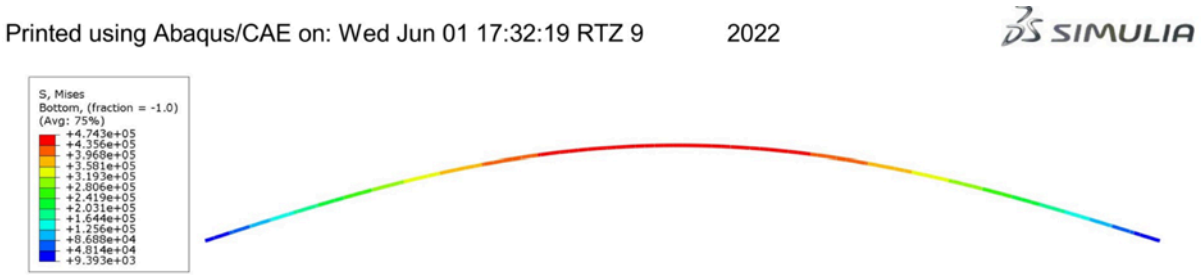

Fig. 3. Equivalent stresses calculated in Abaqus

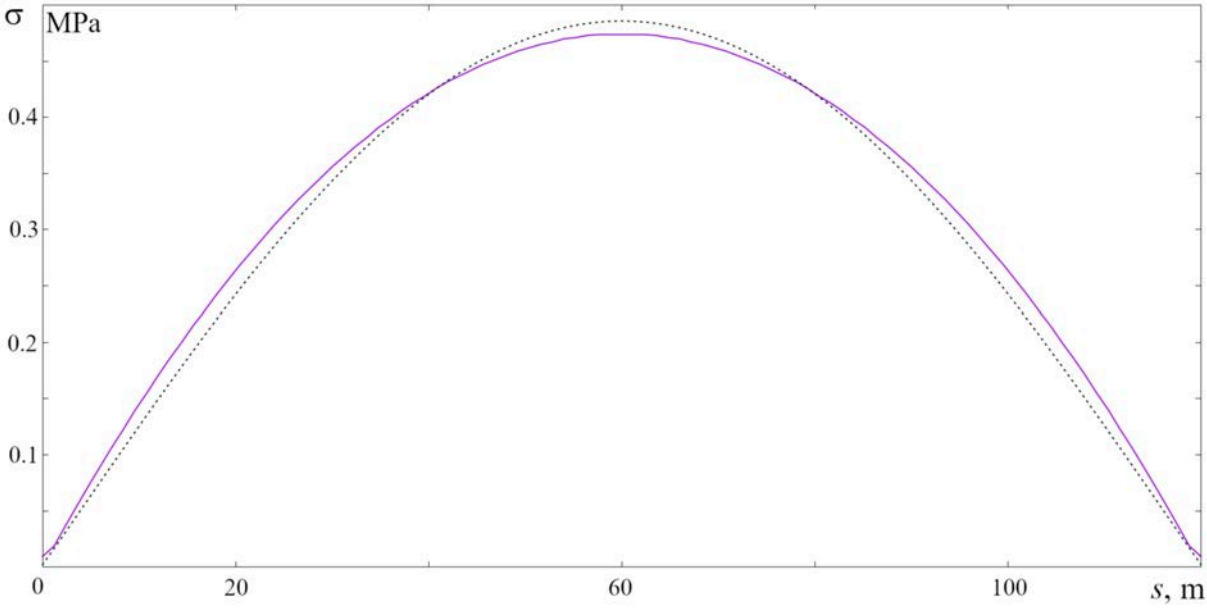

Fig. 4. Exact stress values (dashed line) and numerical solution by FEM (solid line)

In Fig. 4 we can see that the exact and numerical solutions for stresses are in good agreement with each other.

We determine the relative errors for these stresses:

$$\max \varepsilon_{AbNum} = \max \frac{\left|\sigma_{экв} - \left|\sigma_{zh}\right|\right|}{\max\left|\sigma_{экв}\right|},\ \max \varepsilon_{\sigma exact} = \max \frac{\left|\left|\sigma_z\right| - \sigma_{экв}\right|}{\max\left|\sigma_z\right|}.$$

After doing the calculations, we find: $\max \varepsilon_{AbNum} = 0.048$, $\max \varepsilon_{\sigma exact} = 0.0239$.

Thus, the stress found by the model (5) deviates from the solution by the finite element method in CAE Abaqus by no more than 4.8%. On the other hand, the Abaqus system itself gives an error that does not exceed 2.4% for the one-dimensional geometric model we have constructed. It should be noted that the accuracy of the theory of rods and shells does not exceed 5% [26].

Summarizing the solution of *task 1*, we can conclude that the created mathematical model allows us to perform stress calculations in bent pipes with high accuracy. The numerical analysis results are consistent with the known exact and approximate solutions. Restrictions (2) and (3) should be imposed on the parameters of the mathematical model.

Task 2. A comparison is made of the displacement of the axial line of the pipeline according to the proposed mathematical models: the model of a semi-momentless shell in [12] and the model of a bent rod in [11]. Numerical methods of solution are proposed ibid.

Condition (2) is satisfied, which makes it possible to use the shell model (1).A comparison of the dynamics of the center line as the rod and shell is shown in Fig. 5. Figure 5a shows the displacement of the profile when the rod model is chosen, Fig. 5b – when chosen the shell model.

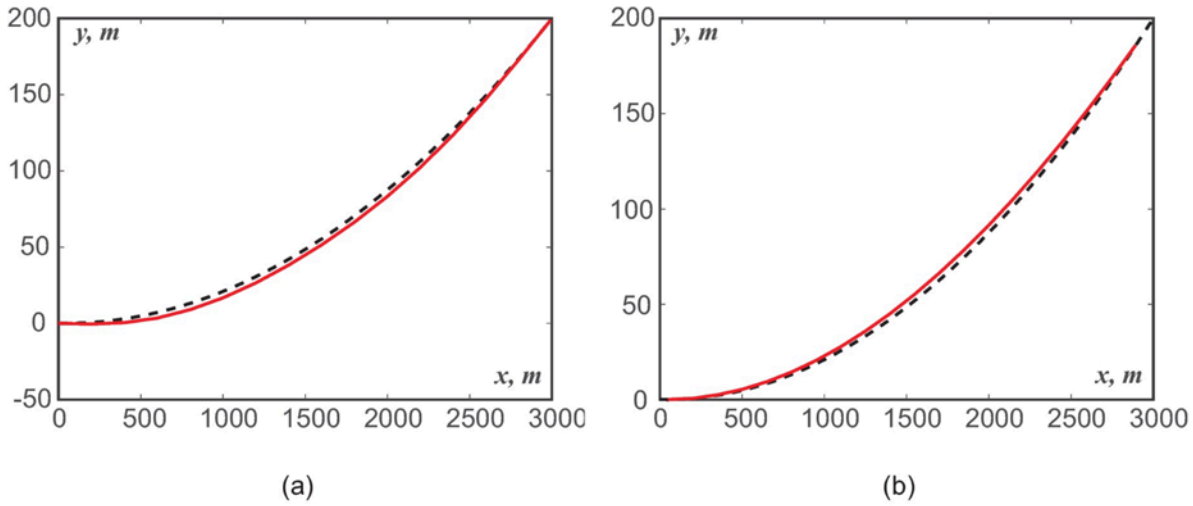

Fig. 5. Pipe displacement: a) rod model; b) shell model

In [28], the phenomenon of "reverse behavior of the pipe" is described, when the centerline moves against the direction of the centrifugal force from the flow. Figure5b shows that the shell model (6) describes this phenomenon. The rod model [11] in this case gives a different behavior of the pipe.

Calculating (8), we find: $E_{irv} \approx 42.4$. The resulting value is significantly less than the value $E_{irv} \geq 286$, at which the rod model is required. This means that the application of the mathematical model [12] as more general is justified.

So, according to *task 2*, we can conclude that our calculations correspond to the results presented in the scientific literature.

7. Conclusion

Comparative analysis of mathematical models of the pipeline is performed, verification of these models based on a comparison of exact and numerical solutions is carried out, and the limits of their applicability are determined.

The formulation of the mathematical model of the pipeline as an elastic shell is given and the basic parameters of this model are determined. The equations of the first approximation with respect to the small curvature parameter are compared for mathematical models of moment and semi-momentless shells. The acting forces and stresses are calculated for the test problem of bending a pipeline segment. Numerical solution to the test problem is found, and the grid functions of stresses and bending moments are calculated on its basis. The geometry and finite element model of a bent pipe under transverse load are constructed in CAE Abaqus. Stresses and bending moments in all approximate models are compared with exact values of these quantities, and numerical values of errors are found. It has been established that the proposed mathematical model makes it possible to find stresses in pipes with high accuracy. It has been established that the proposed mathematical models have areas of applicability confirmed by known scientific data.

References

1. Liu R, Xiong H, Wu X, Yan Sh. Numerical studies on global buckling of subsea pipelines. *Ocean Engineering*. 2014;78: 62-72.
2. Liu R, Wang W, Yan Sh, Wu X. Engineering measures for preventing upheaval buckling of buried submarine pipelines. *Applied Mathematics and Mechanics (Engl. Ed.).* 2012;33(6): 781-796.
3. Feodosiev VI. *Advanced Stress and Stability Analysis: Worked Examples*. Berlin: Springer; 2005.
4. Towhata I. *Geotechnical Earthquake Engineering*. Berlin: Springer; 2008.
5. Bai Y. *Pipelines and Risers*. Amsterdam: Elsevier; 2003.
6. Svetlitsky VA. *Dynamics of Rods*. Berlin: Springer; 2005.
7. Bucalem ML, Bathe KJ. Finite element analysis of shell structures. *Archives of Computational Methods in Engineering*. 1997;4(1): 3-61.
8. Klar A, Marshall AM. Shell versus beam representation of pipes in the evaluation of tunneling effects on pipelines. *Tunnelling and Underground Space Technology*. 2008;23(4): 431-437.
9. Yifei Y, Bing S, Jianjun W, Xiangzhen Y. A study on stress of buried oil and gas pipeline crossing a fault based on thin shell FEM model. *Tunneling and Underground Space Technology*. 2018;81: 472-479.
10. Rukavishnikov VA, Tkachenko OP. Numerical and asymptotic solution of the equations of propagation of hydroelastic vibrations in a curved pipe. *Journal of Applied Mechanics and Technical Physics*. 2000;41: 1102-1110.
11. Rukavishnikov VA, Tkachenko OP. Nonlinear equations of motion of an extensible underground pipeline: derivation and numerical modeling. *Journal of Applied Mechanics and Technical Physics*. 2003;44(4): 571-583.
12. Rukavishnikov VA, Tkachenko OP. Dynamics of a fluid-filled curvilinear pipeline. *Applied Mathematics and Mechanics*. 2018;39(6): 905-922.
13. Rukavishnikov VA, Tkachenko OP. Approximate resolving equations of mathematical model of a curved thin-walled cylinder. *Applied Mathematics and Computation*. 2022;422: 12696.
14. Vlasov VS. *Basic Differential Equations in General Theory of Elastic Shells*. *Technical Memorandum 1241*. Washington: NACA; 1951.

15. Rukavishnikov VA, Tkachenko OP. Mathematical model of the pipeline with angular joint of elements. *Mathematical Methods in the Applied Sciences*. 2020;43(13): 7550-7568.
16. Rukavishnikov VA. Weighted FEM for two-dimensional elasticity problem with corner singularity. *Lecture Notes in Computational Science and Engineering*. 2016;112: 411-419.
17. Rukavishnikov VA, Rukavishnikova EI. On the dirichlet problem with corner singularity. *Mathematics*. 2020;8(11): 1870.
18. Rukavishnikov VA, Mosolapov AO, Rukavishnikova EI. Weighted finite element method for elasticity problem with a crack. *Computers & Structures*. 2021;243: 106400.
19. Bratov VA. Numerical simulations of dynamic fracture. Crack propagation and fracture of initially intact media. *Materials Physics and Mechanics.* 2021;47(3): 455-474.
20. Hover FS, Triantafyllou MS. Linear dynamics of curved tensioned elastic beams. *Journal of Sound and Vibration*. 1999;228(4): 923-930.
21. Tkachenko OP. Comparison of the computational experiment´s results on the two mathematical models of pipeline. *Mathematical modeling, computer and field experiment in natural sciences*. 2018;1. Available from: http://mathmod.esrae.ru/17-59 [Accessed: 23th August 2022]. (In Russian)
22. Loitsyansky LG. *Mechanics of Fluid and Gas*. Moscow: Drofa; 2003. (In Russian)
23. Lavrinenkov AD, Yakimov ID, Levadny EV, Boyko AB, Ostapov AV, Ziginov NV. *SIMULA Abaqus. Solving Applied Problems*. Moscow: TESIS; 2015. (In Russian)
24. Timoshenko SP. *Strength and Vibrations of Structural Elements*. Moscow: Science; 1975. (In Russian)
25. Bronshtein IN, Semendyayev KA. *A Guide Book to Mathematics: Fundamental Formulas, Tables, Graphs, Method*s. Zürich: Springer; 1973.
26. Alexandrov AV, Potapov VD, Derzhavin BP. *Resistance of Materials*. Moscow: Higher School; 2000. (In Russian)
27. Shelofast VV, Chugunova TB. *Fundamentals of machine design. Examples of problem solving.* Moscow: APM; 2007. (In Russian)
28. Athisakul Ch, Monprapussorn T, Pulngern T, Chucheepsakul S. The effect of axial extensibility on three-dimensional behavior of tensioned pipes/risers transporting fluid. In: *Proceedings of the Eighth (2008) ISOPE Pacific/Asia Offshore Mechanics Symposium*. 2008. p.97-104.

THE AUTHORS

Tkachenko O.P.
e-mail: olegt1964@gmail.com
ORCID: 0000-0003-1806-0274